

Reversal of Impurity Pinch Velocity in Tokamaks Plasma with a Reversed Magnetic Shear Configuration

S. Futatani,¹ X. Garbet,² S. Benkadda,¹ and N. Dubuit¹

¹International Institute for Fusion Science, CNRS-Université de Provence, Centre de St. Jérôme, Case 321, 13397 Marseille Cedex 20, France

²Association EURATOM-CEA sur la Fusion Contrôlée, CEA Cadarache, 13108 St. Paul-Lez-Durance, France

(Received 18 July 2009; published 7 January 2010)

Impurity transport in tokamak core plasmas is investigated with a three-dimensional fluid global code. It is shown that, in the presence of an internal transport barrier (ITB) created by a reversed magnetic shear configuration, one can obtain a reversal of the impurity pinch velocity which can change from the inward direction to the outward direction. This scenario is favorable for expelling impurities from the central region and decontaminating the core plasma. The mechanism of pinch reversal is attributed to a change of direction of the curvature pinch and to a modification of the dominant underlying instability caused by a change of the gradient of the ion temperature and consequently of the ITB formation.

DOI: 10.1103/PhysRevLett.104.015003

PACS numbers: 52.25.Fi, 52.35.Ra, 52.55.Fa

Impurity transport is an important issue for the success of the International Thermonuclear Experimental Reactor (ITER) as it can strongly influence the plasma performance. It is important to prevent impurity accumulation in order to maintain stationary plasma conditions [1]. Impurity accumulation is predicted by the theory of collisional transport when the main ion density profile is peaked and thermal screening is negligible [2]. However, the predictions of neoclassical theory are rarely matched exactly by the observations. Turbulent transport is considered as a plausible candidate for explaining this discrepancy.

A standard phenomenology describes the steady state particle flux Γ_s as a sum of a diffusive term and a convective term [3–5]: $\Gamma_s = -D_s \nabla n_s + n_s V_s$, where D_s is the diffusivity, n_s is the density, and V_s is the radial pinch velocity of species “s”. Several mechanisms have been identified in the framework of the quasilinear theory to explain the pinch velocity. First, perpendicular compressibility induces a curvature pinch velocity which is usually directed inward but can change sign with the magnetic shear [6]. Second, parallel compressibility is responsible for a second contribution that depends on the phase velocity of the fluctuations. And finally, the temperature gradient is responsible for a thermodiffusion term which also depends on the phase velocity.

In this Letter, it is shown that an internal transport barrier produced with reversal magnetic shear is a favorable configuration for getting a reversal of the impurity pinch velocity. This is an important issue for a fusion reactor as it allows the decontamination of the core plasma and prevents the degradation of confinement. This property is demonstrated by using 3D global fluid simulations of impurity transport in tokamak core turbulence. These simulations are consistent with the predictions of the quasilinear theory regarding the various contributions to the pinch velocity of impurities.

In the following, we investigate the impurity turbulent transport using a three-dimensional nonlinear global fluid code TRB [7,8] which includes ion temperature gradient (ITG) mode and trapped electron mode (TEM) instabilities. Calculations are performed at a fixed flux; i.e., particle and heat source densities are fixed and profiles of densities, parallel velocities and pressures evolve accordingly without assuming scale separation. Configurations with monotonic or reversed q profile can be studied with the TRB code; q is called the safety factor and it measures the pitch angle of the magnetic field lines. The code solves the evolution equation of density and pressure for three species: deuterium, trapped electrons, and one impurity species. A set of fluid equations is used here to describe a collisionless ITG/TEM turbulence [9]:

$$d_t n_s = -\kappa_s \cdot (n_s \nabla \phi + \nabla p_s / e_s) - \nabla_{\parallel} (n_s v_{\parallel s}), \quad (1)$$

$$d_t p_s = -\kappa_s \cdot (p_s \nabla \phi + \nabla (p_s^2 / n_s) / e_s) - \gamma \nabla_{\parallel} (p_s v_{\parallel s}), \quad (2)$$

$$n_s m_s d_t v_{\parallel s} = -n_s e_s \nabla_{\parallel} \phi - \nabla_{\parallel} p_s. \quad (3)$$

Here, n_s , p_s , $v_{\parallel s}$, ϕ are the density, the pressure, the parallel velocity, and the electric potential, respectively. The labels “s” can be “e”, “i” and “z” which are for trapped electrons, ions, and impurities, respectively. We solve eight equations for n_e , n_z , p_e , p_i , p_z , Ω , $v_{\parallel i}$, and $v_{\parallel z}$. Passing electrons are assumed to be adiabatic, while the dynamics of trapped electrons is described by Eqs. (1)–(3), with $v_{\parallel e} = 0$. The continuity equation for the main ion density n_i is taken into account in a different form: from the ambipolarity relation, one gets instead an equation for the vorticity Ω , $\Omega = f_c n_{e,\text{eq}} \frac{\phi - \langle \phi \rangle}{T_{e,\text{eq}}} - (n_{i,\text{eq}} + A n_{z,\text{eq}} \nabla^2 \phi)$. The curvature drift operator is $\kappa_s = \frac{2}{B} \frac{\mathbf{B}}{B} \times \frac{\nabla B}{B}$ for ion species. For trapped electrons, κ_s is replaced by the precession frequency in the toroidal direction, i.e., $\kappa_s = \frac{1}{BR} (\frac{1}{2} + \frac{4s}{3}) \mathbf{e}_{\varphi}$;

here, e_φ is a unit vector of toroidal direction and R is the plasma major radius. Here, $\hat{s} = (r/q)dq/dr$ is the magnetic shear. The Lagrangian time derivative is defined as $\frac{d}{dt} = \frac{\partial}{\partial t} + \mathbf{v}_E \cdot \nabla - D\nabla^2$, where D is a ‘‘collisional’’ diffusion operator and $\mathbf{v}_E = \frac{\mathbf{B} \times \nabla \phi}{B^2}$ is the electric drift velocity. Note that the perturbed part of $f_i n_e$ is the fluctuating density of trapped electrons, whereas $n_{e,eq}$ is the total equilibrium electron density normalized to n_0 . The adiabatic compression index is $\gamma = 5/3$. The normalization is of the gyro-Bohm type, as referenced in Ref. [7]. The fraction of trapped (respectively, passing) electrons is $f_t = 2/\pi(2r/R)^{1/2}$ (respectively, $f_c = 1 - f_t$).

A common assumption for the impurity flux is a diffusion-convection equation $\Gamma_z = -D_z \nabla n_z + V_z n_z$ [7,10–14]. In steady state conditions and in plasma regions where the source can be neglected, the local logarithmic density gradient of an impurity $1/L_{n_z} = -\nabla n_z/n_z$ is directly related to the ratio of the convection velocity to the diffusion coefficient, V_z/D_z . Hence, the peaking of an impurity density is determined by the ratio $-V_z/D_z$, or equivalently the normalized peaking factor $-RV_z/D_z$. The peaking factor profile is an important parameter to characterize the impurity density pinch.

The diffusion-convection expression of the flux is consistent with the quasilinear theory. Indeed the radial turbulent flux of species s is $\Gamma_s = \langle n_s \mathbf{v}_E \rangle = \sum_{k,\omega} n_{s,k\omega} \frac{ik_\theta}{B_{eq}} \tilde{\phi}_{k\omega}^*$. Replacing the density by its linear response in this expression, one finds the quasilinear flux:

$$\Gamma_s = \sum_{k,\omega} \frac{1}{N} \frac{e_s}{T_{s,eq}} \frac{ik_\theta}{B} |\tilde{\phi}_{k,\omega}|^2 \{-F\omega_{ns}^* - G\omega_{ps}^* + FG + \gamma G^2\} n_{s,eq}, \quad (4)$$

where $F = \omega - 2\gamma\omega_{ds} - \gamma\frac{\omega_{\parallel}^2}{\omega}$, $G = \omega_{ds} + \frac{\omega_{\parallel}^2}{\omega}$, and $N = \omega F + \gamma\omega_{ds}G$. The curvature drift frequency is defined as $\omega_{ds} = k_y \frac{2T_{s,eq}}{e_s B R} \lambda_{\hat{s}}$, where $\lambda_{\hat{s}} = \langle \cos\theta + \hat{s}\theta \sin\theta \rangle$. The bracket is an average of the bounce motion for trapped particles, or the average of poloidal mode structure for passing particles. The diamagnetic density and pressure frequencies are defined as $\omega_{ns}^* = k_\theta \frac{T_{s,eq}}{e_s B} \frac{dn_{s,eq}}{n_{s,eq} dr}$, $\omega_{ps}^* = k_\theta \frac{T_{s,eq}}{e_s B} \frac{dP_{s,eq}}{P_{s,eq} dr}$, and the parallel transit frequency as $\omega_{\parallel} = k_{\parallel} \sqrt{\frac{T_{s,eq}}{m_s}}$.

The first term in Eq. (4), proportional to $\nabla_r n_{eq}$, corresponds to the diffusive part of the flux. The other terms are referred to as pinch velocities. To identify the mechanisms underlying the pinch velocity, we assume now that one mode is dominant, and that the following ordering $\omega_{ps}^* \gg \omega \gg \omega_{ds} \gg \omega_{\parallel}$ holds. This ordering is consistent with the interchange character of ITG/TEM turbulence and the fluid approximation. Then it appears that the pinch velocity is the sum of three components. The first one, called curvature pinch, gives a peaking factor that mainly depends on

the geometry, $\frac{V_{cur} R}{D} \sim -2\lambda_{\hat{s}}$ [10–12]. It is caused by compressibility of the $\mathbf{E} \times \mathbf{B}$ drift velocity in an inhomogeneous magnetic field. This effect is related to turbulent equipartition (TEP) effect [15,16]. In particular, the ratio VR/D is proportional to the parameter $\lambda_{\hat{s}}$, which also characterizes the canonical profile $\exp\{-\frac{2}{R} \int^r \lambda_{\hat{s}}(r') dr'\}$. For trapped electrons, $\lambda_{\hat{s}}$ is related to the precessional frequency, thus depends on magnetic shear. For impurities, $\lambda_{\hat{s}}$ depends on \hat{s} when modes are strongly ballooned. We note that TEP effects also exist for momentum pinch [15,16]. When the curvature pinch velocity is proportional to the magnetic shear, it is inward for a monotonic increasing q profile and outward for reversed q profile. It is independent of charge and mass. The second pinch velocity, called thermodiffusion is such that $\frac{V_{VT,R}}{D} \sim \frac{2\lambda_{\hat{s}} \omega_{ps}^*}{\omega - 2\gamma\omega_{ds}}$ [11,13]. It originates from the compression of the diamagnetic drift velocity and is proportional to the impurity

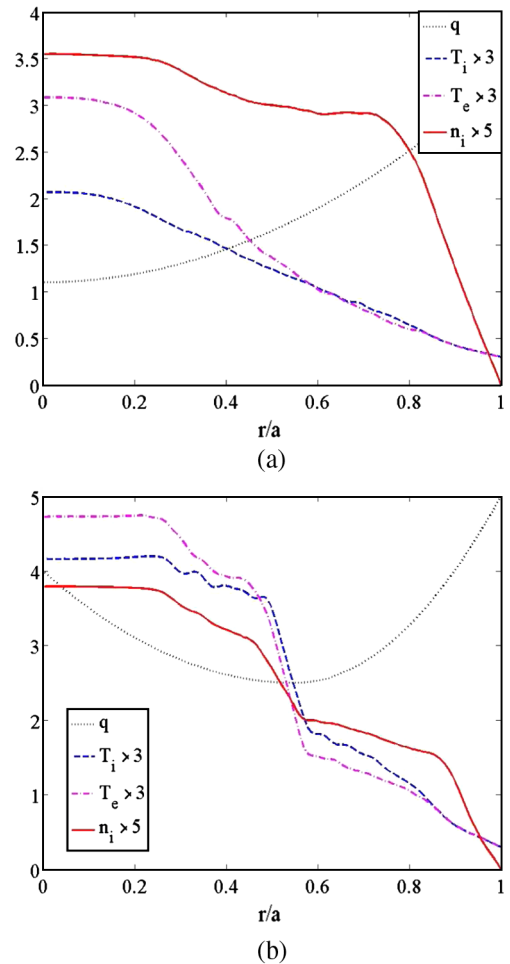


FIG. 1 (color online). Radial dependence of (a) a monotonic safety factor and (b) a reversed safety factor. A strong barrier is created in the reversed magnetic shear case (b). The position of zero shear is $\rho_{min} = 0.55$ for the reversed magnetic shear case. The ion temperature, the electron temperature, and the ion density profiles are also plotted.

pressure gradient. Its magnitude is inversely proportional to the charge number. As a result the thermodiffusion pinch becomes negligible for high Z impurity [7]. The third contribution to the pinch velocity is connected with the parallel dynamics of the impurities, $\frac{V_{\parallel cs} R}{D} \sim -2\lambda_{\delta} \frac{\omega_{\parallel}^2}{\omega\omega_{ds}}$ [14]. The magnitude of this pinch depends on the ratio Z/A and thus depends weakly on the impurity characteristics in realistic cases. The thermodiffusion pinch and the pinch linked to the parallel compressibility can change sign depending on the direction of propagation of the fluctuations. The thermodiffusion pinch is inward for transport driven by instabilities rotating in the electron diamagnetic direction, such as TEM, and outward for transport driven by instabilities rotating in the ion diamagnetic direction such as ITG. In contrast, the pinch originating from the compression of parallel velocity has the opposite variation. Therefore, the total pinch, which is the sum of at least these three mechanisms, has a dependence on Z that is different depending whether instabilities rotate in the ion or the electron diamagnetic direction. The relative magnitude of these mechanisms can change depending on plasma conditions, such as q profile, or impurity temperature gradient. Nevertheless, the dependence on Z is usually weak since the curvature pinch velocity is the dominant contribution.

Various simulations have been performed to investigate the basic properties of impurity transport in core plasma ITG/TEM turbulence with and without ITBs. The simulated impurities are helium (He, $Z = 2$, $A = 4$). As shown in Fig. 1, ITBs are produced with a reversed q profile. The barrier onset is sensitive to the value of q_{\min} [17] but not on q_0 in contrast with recent experimental observations [18].

Impurities are injected in a steady turbulence. Injecting impurities in the plasma edge leads to a transient that can be used to determine the transport coefficients. Figure 2 shows the scatter plot of Γ_z/n_z against $\nabla n_z/n_z$. A linear fit provides the values of the diffusion coefficient D_z and the convection velocity V_z . The good quality of the fit indicates

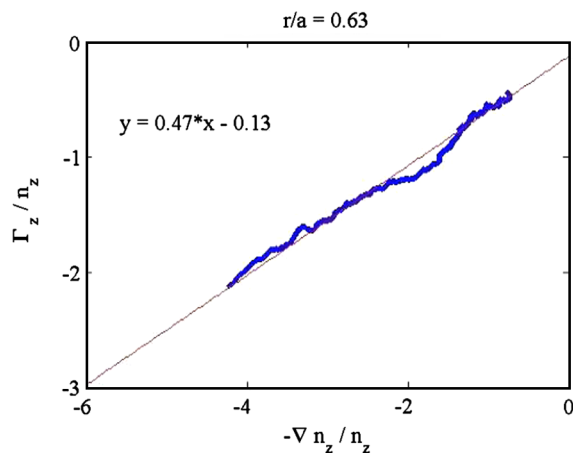


FIG. 2 (color online). Scatter plot of Γ_z/n_z versus $\nabla n_z/n_z$ for helium in reversed q profile. The solid line is the linear fit.

that a simple diffusion-convection velocity model is robust, even in the strongly nonlinear regime.

Knowing the values of the diffusion coefficients and pinch velocity, one can test the prediction of the quasilinear theory for various q profiles. Let us note that three terms contribute to the right-hand side of Eq. (1): $-\kappa_{\delta} \cdot (n_s \nabla \phi)$ which is related to curvature pinch, $-\kappa_{\delta} \cdot (\nabla p_s / e_s)$, which is the thermodiffusion contribution, and the parallel compressibility term $-\nabla_{\parallel}(n_s v_{\parallel s})$. Each of these three terms can be switched on or off in the numerical simulations for the impurity species ($s = z$). It can be shown from quasilinear theory that switching on one of these terms, and the others off, provide the corresponding contribution to the pinch velocity. This gives a way to compute numerically each contribution to the pinch velocity. Figure 3 shows the diffusion coefficients D_z and the pinch velocity V_z for each case. The total pinch velocity is labeled V_z , $V_{\perp cz}$ stands for the curvature pinch, the thermodiffusion pinch is $V_{\nabla Tz}$, and the parallel compressibility pinch is noted $V_{\parallel cz}$. The radial profile of the turbulent diffusion coefficient D_z are shown in Figs. 3(a) and 3(b), respectively. Figure 3(a) shows that the diffusion coefficient D_z in the barrier is strongly reduced. The barrier region is $0.45 < r/a < 0.62$. Figures 3(c) and 3(d) show the radial profiles of various components of the pinch velocities. We observe that the curvature pinch velocity $V_{\perp cz}$ is directed inward in the case of monotonic q profile (without ITB), as shown in Fig. 3(d). When the magnetic shear is negative, the direction of the curvature pinch velocity in the core region ($r/a < 0.45$) is opposite to the one obtained for monotonic q profile, i.e., is in the outward direction as shown in Fig. 3(c). This is consistent with the quasilinear theory

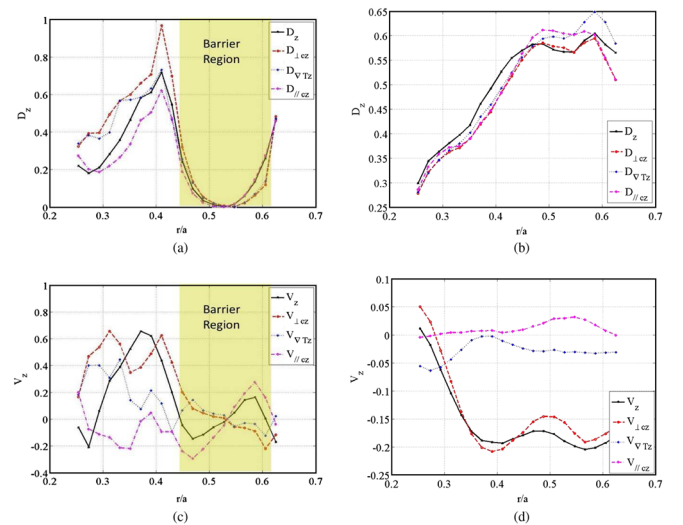


FIG. 3 (color online). Radial profile of (a) the turbulent diffusion coefficient D_z and (c) turbulent pinch velocity V_z for helium in magnetic shear reversal. The radial profile of (b) the turbulent diffusion coefficient D_z and (d) the pinch velocity V_z in monotonic q profile.

TABLE I. Direction of the curvature pinch velocity $V_{\perp cz}$, the thermodiffusion pinch velocity $V_{\nabla Tz}$, and the parallel compressibility pinch velocity $V_{\parallel cz}$ for ITG and TEM cases.

Pinch type	TEM	ITG
$V_{\perp cz}$	Inward ($\hat{s} > 0$) Outward ($\hat{s} < 0$)	Inward ($\hat{s} > 0$) Outward ($\hat{s} < 0$)
$V_{\nabla Tz}$	Inward	Outward
$V_{\parallel cz}$	Outward	Inward

which predicts a curvature pinch proportional to $\nabla q/q$. The curvature pinch provides the main contribution to the total velocity so that the latter is mainly directed outward. In the barrier region ($0.45 < r/a < 0.62$), the turbulence intensity is small. Therefore, it is not expected that quasilinear theory applies. This is why the pinch velocity changes sign and is directed outward (inward) when magnetic shear is positive (negative).

The thermodiffusion pinch $V_{\nabla Tz}$ is negative for monotonic q profile and reverses its sign when the magnetic shear is reversed. The parallel compressibility pinch $V_{\parallel cz}$ behaves in the opposite way, i.e., is positive for monotonic q profile and negative for reversed q profile. This is consistent with the turbulence dominated by TEM for monotonic q profile and by ITG modes for reversed q profile. The calculation of the inverse gradient length $\nabla T_e/T_e$ shows that it is twice larger for monotonic than for reversed q profile. The other inverse gradient lengths $\nabla T_i/T_i$ and $\nabla n_e/n_e$ are less affected. This suggests that the simulation with monotonic q profile is more prone to TEM turbulence. This analysis is supported by linear stability analysis which shows that the phase velocity of drift waves changes its sign when the q profile is changed. We note that the sum of the three contributions to the pinch velocity does not match exactly the total velocity, in particular, for the case with magnetic shear reversal. This could be due to some breakdown in the ordering that is needed for this result to apply, or to a departure from the quasilinear theory prediction. Other impurities (beryllium, boron, nitrogen, neon, argon, krypton, and tungsten, for instance) have been simulated and give consistent results.

Table I gives a summary table which is computed with a quasilinear theory. We observe that the results of Fig. 3 agree with the quasilinear prediction of Table I. Hence the simulations agree with quasilinear theory predictions for all configurations. Moreover, it appears that the negative magnetic shear is favorable as it leads to an impurity decontamination.

In summary, impurity turbulent transport has been studied in configurations with positive and negative magnetic shear. This has been done by developing a quasilinear theory that accounts for compressibility effects and ther-

modiffusion. In addition, 3D fluid simulations have been performed. This simulation shows that the predictions of the quasilinear theory are robust. In particular it is found that the curvature pinch is the main component in monotonic q profiles, hence leading to an impurity peaking. However, reversed q profile leads to the reversal of curvature pinch velocity which becomes outward. The sign of the thermodiffusion and parallel compressibility pinch velocities changes with the phase velocity of fluctuations, i.e., depends on the underlying instability (ITG or TEM). These velocities are subdominant in the monotonic q profile, but play a significant role in the reversed q profile. It appears that the magnetic shear is the main control parameter and a negative value is favorable for the plasma decontamination in the core. This effect should partially balance the detrimental neoclassical inward pinch effect which may appear in the barrier [19].

The authors are grateful to Dr. C. Bourdelle, Dr. R. Guirlet, and Dr. D. Villegas for very helpful and stimulating discussions.

-
- [1] ITER Physics Expert Groups on Confinement and Transport and Confinement Modelling and Database, Nucl. Fusion **39**, 2175 (1999).
 - [2] S. P. Hirshman and D. J. Sigmar, Nucl. Fusion **21**, 1079 (1981).
 - [3] B. Coppi and C. Spight, Phys. Rev. Lett. **41**, 551 (1978).
 - [4] W. M. Tang, G. Rewoldt, and L. Chen, Phys. Fluids **29**, 3715 (1986).
 - [5] P. W. Terry, Phys. Fluids B **1**, 1932 (1989).
 - [6] L. Garzotti *et al.*, Nucl. Fusion **46**, 994 (2006).
 - [7] N. Dubuit *et al.*, Phys. Plasmas **14**, 042301 (2007).
 - [8] X. Garbet and R. E. Waltz, Phys. Plasmas **3**, 1898 (1996).
 - [9] J. Weiland, *Collective Modes in Inhomogeneous Plasmas and Advanced Fluid Theory*, IOP Series in Plasma Physics (Taylor & Francis, London, 1999).
 - [10] M. B. Isichenko, A. V. Gruzinov, and P. H. Diamond, Phys. Rev. Lett. **74**, 4436 (1995).
 - [11] X. Garbet *et al.*, Phys. Rev. Lett. **91**, 035001 (2003).
 - [12] C. Estrada-Mila, J. Candy, and R. E. Waltz, Phys. Plasmas **12**, 022305 (2005).
 - [13] C. Angioni *et al.*, Phys. Plasmas **10**, 3225 (2003).
 - [14] C. Angioni and A. G. Peeters, Phys. Rev. Lett. **96**, 095003 (2006).
 - [15] T. S. Hahm *et al.*, Phys. Plasmas **14**, 072302 (2007).
 - [16] O. Gurcan *et al.*, Phys. Plasmas **14**, 042306 (2007).
 - [17] X. Garbet *et al.*, Phys. Plasmas **8**, 2793 (2001).
 - [18] F. Turco *et al.*, Plasma Phys. Controlled Fusion **51**, 065021 (2009).
 - [19] H. Takenaga *et al.*, Nucl. Fusion **43**, 1235 (2003); R. Dux *et al.*, Nucl. Fusion **44**, 260 (2004); P. C. Efthimion *et al.*, Phys. Plasmas **5**, 1832 (1998).